



Open access

This is not the published version of the article / Þetta er ekki útgáfa útgáfa greinarinnar

Author(s)/Höf.: D. B. Gophane; B. Endeward; T. F. Prisner; S. Th. Sigurdsson

Title/Titill: A semi-rigid isoindoline-derived nitroxide spin label for RNA

Year/Útgáfuár: 2018

Version/Útgáfa: Post – print / Lokaútgáfa höfundar

Please cite the original version:

Vinsamlega vísið til útgefnu greinarinnar:

Gophane, D. B., Endeward, B., Prisner, T. F., & Sigurdsson, S. T. (2018). A semi-rigid isoindoline-derived nitroxide spin label for RNA. *Organic and Biomolecular Chemistry*, 16(5), 816-824.
doi:10.1039/c7ob02870a

Rights/Réttur: © The Royal Society of Chemistry 2018

A semi-rigid isoindoline-derived nitroxide spin label for RNA

Dnyaneshwar B. Gophane,^[a] Burkhard Endeward,^[b] Thomas F. Prisner^{*[b]} and Snorri Th. Sigurdsson^{*[a]}

Received 00th January 20xx,
Accepted 00th January 20xx

DOI: 10.1039/x0xx00000x

www.rsc.org/

A new isoindoline-derived benzimidazole nitroxide spin label, ImUm, was synthesized and incorporated into RNA oligoribonucleotides. ImUm is the first example of a conformationally unambiguous spin label for RNA, in which the nitroxide N-O bond lies on the same axis as the single bond used to attach the rigid isoindoline-based spin label to a uridine base. This results in minimal displacement of the nitroxide upon rotation of this single bond, which is a useful property for a label to be used for distance measurements. Continuous-wave (CW) EPR measurements of RNA duplexes containing ImUm indicate a restricted rotation around this single bond, presumably due to an intramolecular hydrogen bond between the benzimidazole N-H and O4 of the uracil. Orientation-selective pulsed electron-electron double resonance (PELDOR, also called double electron-electron resonance, or DEER) distance measurements between two spin labels in two RNA duplexes showed in one case a strong orientation dependence, further confirming the restricted motion of the spin labels in RNA duplexes.

Introduction

RNA is a ubiquitous family of biopolymers that have multiple vital roles in the coding, decoding, regulation and expression of genes.¹⁻³ The understanding of RNA, DNA and protein function, including their interactions with other molecules, requires knowledge of their respective molecular structures and conformational dynamics. EPR spectroscopy is a useful technique to extract such information.⁴⁻¹⁰ It requires small amounts of material and can be used to study biopolymers under biologically relevant conditions. Since RNA is diamagnetic, paramagnetic groups, or spin labels, must be incorporated at specific sites, a technique referred to as site-directed spin labeling (SDSL).¹¹⁻¹⁴ Apart from a recent report of noncovalent and site-specific spin-labeling of RNA, based on binding of a spin-labeled guanine to an abasic site in duplex RNA,¹⁵ there are two strategies that have been used to incorporate spin labels into RNA using covalent bonds. One is *via* postsynthetic labeling of pre-functionalized sites.¹⁶⁻²³ The other covalent-labeling approach is the phosphoramidite method, in which the spin label is incorporated into the desired oligomer during the oligonucleotide synthesis.²⁴ This approach has the advantage that spin labels with limited flexibility can be incorporated into the oligoribonucleotides. One such label is ζ m,²⁴ a ribonucleotide derivative of the rigid spin label ζ ,²⁵⁻²⁸ (Figure 1), which has been used to probe mono- and

bimolecular RNA structures and measurements of distances and orientation within RNA.²⁹

We have previously reported the conformationally restricted isoindoline-derived benzimidazole spin label ${}^{\text{Im}}\mathbf{U}$ (Figure 1) for DNA, which showed EPR-based spectroscopic properties similar to that of the rigid spin label ζ .³⁰ The restricted mobility was believed to arise, at least in part, from an intramolecular hydrogen bond between the NH of the benzimidazole and O4 of the uracil base.³⁰ ${}^{\text{Im}}\mathbf{U}$ has been used for distance measurements in duplex DNAs and showed a strong orientation dependence, another indication of limited mobility.³¹ Aside from the orientation dependence of ${}^{\text{Im}}\mathbf{U}$, the single bond that connects the benzimidazole moiety to the base lies on an axis that runs through the N-O bond of the nitroxide (Figure 1), which makes ${}^{\text{Im}}\mathbf{U}$ useful for precise distance measurements.

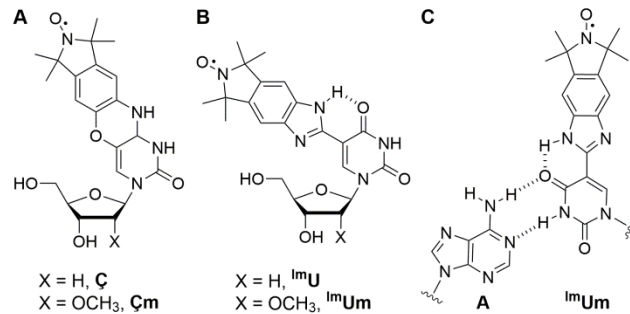


Fig. 1. ζ and ζ m (A), ${}^{\text{Im}}\mathbf{U}$ and ${}^{\text{Im}}\mathbf{Um}$ (B), and base-pairing of ${}^{\text{Im}}\mathbf{Um}$ with adenine (C).

[a]University of Iceland, Department of Chemistry, Science Institute, Dunhaga 3, 107 Reykjavik, Iceland.

[b]Institute of Physical and Theoretical Chemistry, J. W. Goethe University, Max-von-Laue-Str. 7, D-60438 Frankfurt, Germany

† Footnotes relating to the title and/or authors should appear here.

Electronic Supplementary Information (ESI) available: [details of any supplementary information available should be included here]. See DOI: 10.1039/x0xx00000x

solid-phase synthesis. The new label was well tolerated in the A-form helices when paired with adenosine (**Figure 1**), as judged by its small effect on the thermodynamic stability of the labeled RNAs. **^lmUm** showed very limited mobility in duplex RNA, indicating that rotation around the single bond, linking the spin label to the uracil, is indeed restricted. CW-EPR spectroscopy was used to show that the **^lmUm** was able to report on the local environment of the labeling site. PELDOR distance measurements on RNA duplexes using **^lmUm** were in close agreement with distances derived from molecular modeling. Furthermore, PELDOR measurements of **^lmUm**-labeled RNA duplexes showed orientation dependence, further confirming the limited motion of this spin label in RNA duplexes.

Results and discussion

Synthesis and incorporation of **^lmUm** into RNA

The synthesis of **^lmUm** (**Scheme 1**) began with iodination of 2'-O-methyluridine (**Um**).³² The 3'- and 5'-hydroxyl groups of **1** were protected by TBDSMS to give **2**,³³ which was treated with vinyl acetate in the presence of $\text{Pd}(\text{OAc})_2$ to yield the 5-vinyl functionalized compound **3** in good yield.³³ Compound **3** was subjected to dihydroxylation using OsO_4 and *N*-methylmorpholine *N*-oxide (NMO) to obtain the corresponding diol,³⁴ which was further treated with NaIO_4 to give the desired aldehyde **4** in good yield.³⁵ Aldehyde **4** was treated with diamino-tetramethylisoindoline **5** and $\text{K}_3\text{Fe}(\text{CN})_6$, yielding the imidazole derivative **6**. Compound **6** was subjected to m-CPBA-mediated oxidation in the presence of NaN_3 ,³⁰ which presumably adds transiently to the 6-position of the pyrimidine base,³⁶ generating compound **7**. The TBDSMS protecting groups of **7** were removed using TBAF to afford the nucleoside **^lmUm**, followed by tritylation and phosphorylation to give phosphoramidite **9** in good

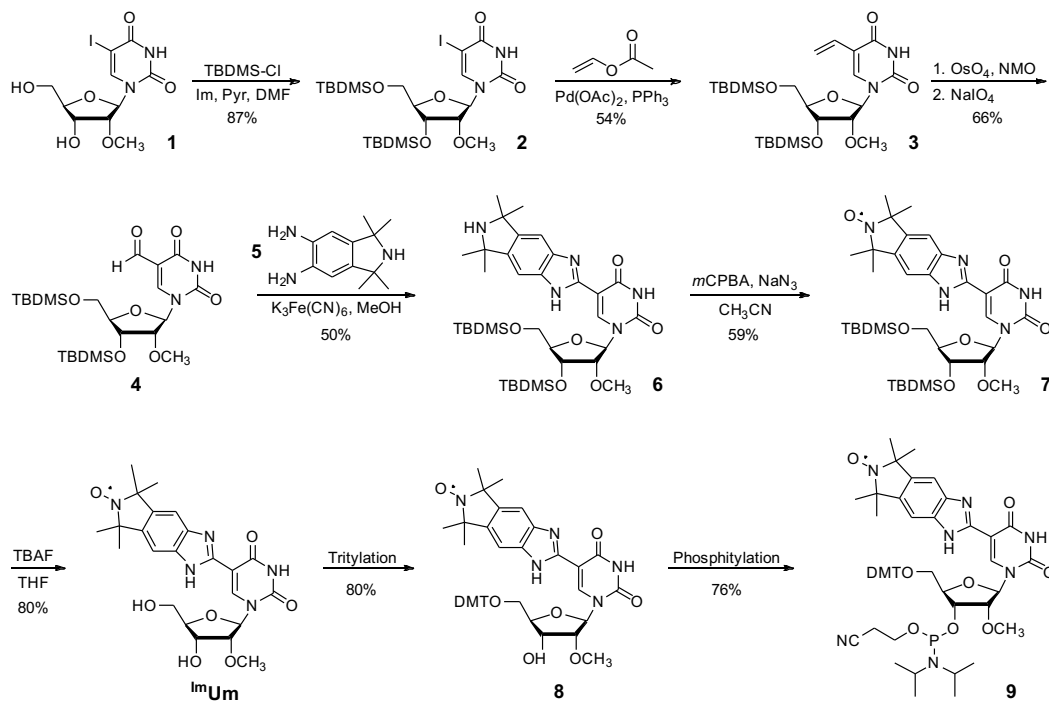
Syntheses and purification of RNA oligonucleotides containing **^lmUm**

^lmUm was incorporated into RNA oligoribonucleotides by solid phase synthesis using the previously reported protocol, with a slight modification.^{24,26} Upon completion of the synthesis, the oligoribonucleotides were cleaved from the solid support and the nucleobases and phosphodiesters were deprotected in a 1:1 mixture of 33% aqueous NH_3 and 8 M MeNH_2 in EtOH. The 2'-O-TBDSMS groups were removed by treatment with $\text{Et}_3\text{N}\bullet 3\text{HF}$, after which water was added and the oligoribonucleotides precipitated with n-butanol. The crude oligoribonucleotides were purified by DPAGE and quantified using UV absorbance spectroscopy.

The effect of **^lmUm** on RNA duplex stability

The incorporation of **^lmUm** into RNA was first demonstrated by synthesis of the 14-mer oligoribonucleotide 5'-(CACGA^lmUmGCGAGGUC). After annealing to a complementary RNA, a thermal denaturation experiment of the duplex 5'-(CACGA^lmUmGCGAGGUC)•5'-(GACCUCGCAUCGUG) (**II**) showed a single melting transition, lowering the melting temperature (T_M) by 6.1 °C compared to the unmodified duplex (**I**) (**Table 1**, **Figure S1A**). We have previously observed a lowering in T_M by 4.0 °C when **^lUm** was incorporated into the center of a 14-mer DNA.³⁰ CD spectra of the **^lmUm**-modified and unmodified oligoribonucleotides were almost identical, confirming that **^lmUm** is well tolerated in an A-form RNA helix (**Figure S1B**).

The spin-label **^lmUm** was also incorporated into the stem region of an RNA hairpin 5'-(G^lmUmCGACGGAAGUCGACAGUA) (**IV**), which contains a six base-pair helix and a stable GGAA tetraloop. In hairpin **IV**, the location of the label is close to the end of the stem and as



Scheme 1. Synthesis of the nucleoside **^lmUm** and its corresponding phosphoramidite (**9**).

yield.

expected, it showed only a minor effect on the T_M (-0.5 °C), compared

to the corresponding unmodified hairpin (**III**) (**Table 1, Figure S1C**). ^{l_m}**Um**-modified hairpin **IV** was annealed to its complementary RNA strand, 3'-(CAGCUGCCUUGAGCUGUCAU), yielding duplex **VIII**, thus placing the label close to the end of the duplex and resulting in only minor destabilization (-0.7 °C) (**Table 1, Figure S1E**). ^{l_m}**Um** was also incorporated into the overhang region of the oligoribonucleotide hairpin **VI**, where it stabilized the hairpin by 3.7 °C, compared to the unmodified hairpin **V** (**Table 1, Figure S1D**). When hairpin **VI** was annealed to its complementary strand, the resulting duplex (**IX**) was stabilized by 2.7 °C (**Table 1, Figure S1F**), relative to the unmodified sequence (**VII**).

Table 1. Sequences and T_m s of RNA hairpins and duplexes

RNA	Sequence	T_m	ΔT_m
I	5' CACGAUGCGAGGU C GUGCUCAGCUCCAG	73.4 ± 0.6	
II	5' CACGA ^{l_m} Um GCGAGGU C GUGC U A CGCUCCAG	67.3 ± 0.3	- 6.1
III	A GUCGACAGUA G CAGCUG ^{5'}	85.2 ± 1.0	
IV	A GUCG A CAGUA G CAGC ^{l_m} Um G ^{5'}	84.7 ± 0.3	- 0.5
V	C GUCGAC U CAGCUGUCAU ^{5'}	76.0 ± 0.5	
VI	C GUCGAC U CAGCUG ^{l_m} Um CAU ^{5'}	79.7 ± 0.3	+ 3.7
VII	5' GUCGACGGAAAGUCGACAGUA CAGCUGCCUUCAGCUGUCAU	74.5 ± 1.0	
VIII	5' G ^{l_m} Um CGACGGAAAGUCGACAGUA C A GCUGCCUUCAGCUGUCAU	73.8 ± 0.8	- 0.7
IX	5' GUCGACGGAAAGUCGAC A GUA CAGCUGCCUUCAGCUG ^{l_m} Um CAU	77.2 ± 0.8	+ 2.7

4 mM duplex in 10 mM sodium phosphate, 100 mM NaCl, 0.1 mM Na₂EDTA, pH 7.0. T_m is the melting temperature and ΔT_m is the difference in T_m between unmodified and modified duplexes.

CW-EPR analyses of ^{l_m}**Um** in duplexes and hairpins

To evaluate the mobility of ^{l_m}**Um** in RNA, we recorded the CW-EPR spectra of the nucleoside ^{l_m}**Um**, the ^{l_m}**Um**-labeled 14-mer RNA single strand and the corresponding 14-mer RNA duplex **II** (**Figure 2**). The nucleoside showed three sharp lines (**Figure 2A**) that broadened upon incorporation into the 14-mer oligoribonucleotide 5'-(CACGA^{l_m}**Um**GCGAGGU) (**Figure 2B**). Upon annealing to its complementary strand 5'-(GACCUCGCAUCGUG), the CW-EPR spectrum showed a splitting of the high- and low-field components (**Figure 2C**), similar to the previously reported rigid spin labels ζ ²⁵ and ζm ,²⁴ as well as to the semi-rigid ^{l_m}**U**.³⁰ Such broadening is characteristic for the slow-motion regime of nitroxide radicals.²⁴

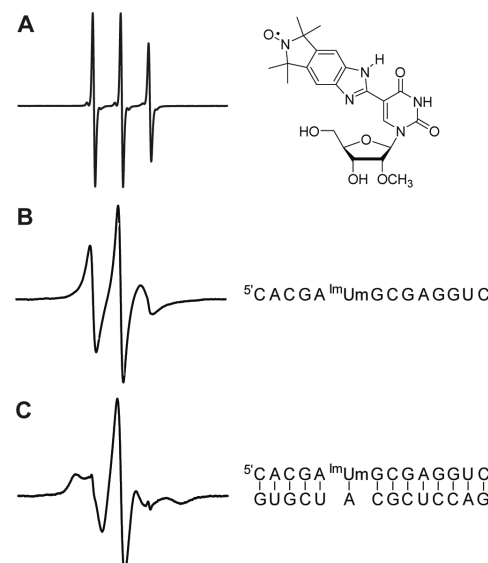


Fig. 2 EPR spectra of ^{l_m}**Um** (**A**), the 14-mer RNA single strand 5'-(CACGA^{l_m}**Um**GCGAGGU) (**B**) and the duplex 5'-(CACGA^{l_m}**Um**GCGAGGU)•5'-(GACCUCGCAUCGUG) (**II**) (**C**). EPR spectra were recorded at 20 °C in a phosphate buffer (10 mM, pH 7.0) containing NaCl (100 mM) and Na₂EDTA (0.1 mM).

To investigate the mobility of the ^{l_m}**Um** in different structural contexts, it was incorporated into RNA hairpins and duplexes (**Figure 3**). The ^{l_m}**Um**-labeled hairpins **IV** (**Figure 3A**) and **VI** (**Figure 3B**) exhibited broadened CW-EPR spectra, compared to single strands. However, spectral line-broadening of hairpin **VI** is less pronounced than hairpin **IV**, since the label is located in the overhang region of hairpin **VI**. The ^{l_m}**Um**-labeled duplexes **VIII** and **IX** showed additional broadening of the spectra, compared to the hairpins. This is presumably due to the increased size of the RNA and the associated slower rotational correlation times, as has been observed with the rigid spin label ζm .²⁴ The EPR spectrum of **IX** at 20 °C is slightly broader than for duplex **VII** (**Figure 3**), presumably because the spin label is farther from the duplex end, where base pairs are more dynamic.^{37,38}

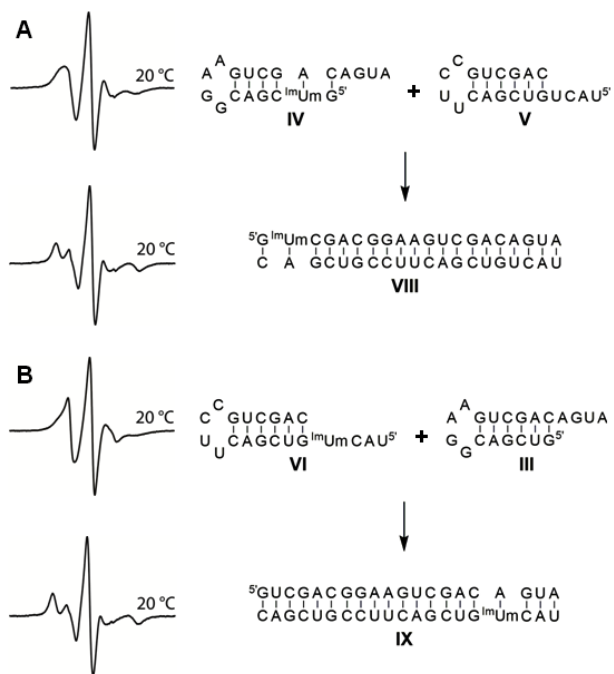
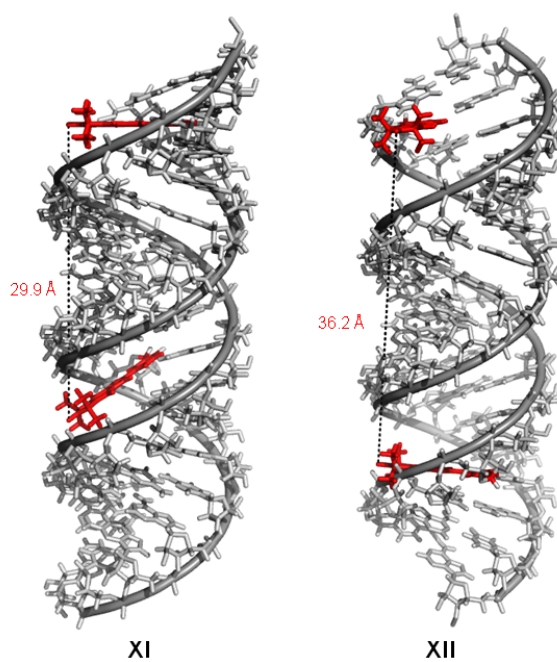


Fig. 3 EPR spectrum of the hairpin **IV** and the spectrum after annealing **IV** to the complementary hairpin **V** to form duplex **VIII** (**A**). EPR spectrum of the hairpin **VI** and the spectrum after annealing **V** with the complementary hairpin **III** to form duplex **IX** (**B**). EPR spectra were recorded at 20 °C in 10 mM phosphate buffer (pH 7.0) containing NaCl (100 mM) and Na₂EDTA (0.1 mM).



(G^{lum}UmCGACGGAAAG^{lum}UmCGACAGUA)• 3'-(CAGCUGCCUUGAGCUGUCAU), left) or 13 base-pairs apart (duplex XII, 5'(G^{lum}UmCGACGGAAAGUCGACAGUA)•3'(CAGCUGCCUUGAGCUG^{lum}UmCAU), right).

Distance measurements of ^{lum}Um-labeled RNAs by PELDOR

Two doubly ^{lum}Um-labeled RNA duplexes were prepared for distance measurements, one containing nine base pairs (**XI**) and the other fourteen base pairs (**XII**) between the spin labels (**Figure 4**). Both the distances between the two spin-label pairs and their relative orientations were different in these duplexes. Orientation selective PELDOR²⁷ was performed at X-Band frequencies in which the pump frequency coincided with the cavity resonance maximum as well as the maximum in spectral density of the nitroxide spectrum. The detection was performed with different frequency offsets on the high frequency side, relative to the pump frequency. For both RNAs, the PELDOR time traces of each offset were different from each other (**Figure 5**). This is a strong indication of orientation dependence resulting from limited mobility of the spin labels within the duplexes. The orientation dependence is very clear, in particular for RNA **XII**. However, in the case of RNA **XI**, the orientation dependence is not as clear, but the differences between the time traces are evident. For each duplex, the different time traces were added to get an average time trace, which removes the orientation effects. DeerAnalysis³⁹ of these time traces yielded the distance distribution shown in **Figure 5**. The measured distances between the spin labels in RNAs **XI** (32.2 Å) and **XII** (38.5 Å) was close to that of the modelled distances (29.9 Å and 36.2 Å, respectively).

Fig. 4 Spartan-derived molecular models of RNA duplexes containing two ^{lum}Um spin labels, placed either nine base-pairs apart (duplex **XI**, 5'-

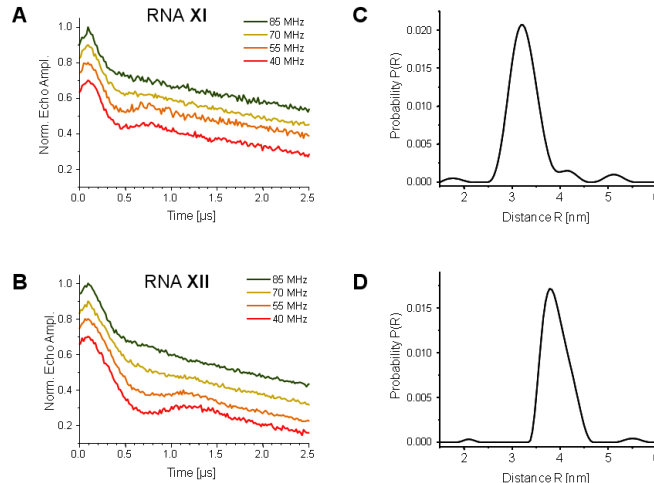


Fig. 5. PELDOR time traces at different frequency offsets for duplex XI 5'(G^{lum}UmCGACGGAAAG^{lum}UmCGACAGUA)•3'(CAGCUGCCUUGAGCUGUCAU) (**A**) and duplex XII 5'(G^{lum}UmCGACGGAAAGUCGACAGUA)•3'(CAGCUGCCUUGAGCUG^{lum}UmCAU) (**B**). Evaluation of interspin distances in doubly spin-labeled RNA duplexes from average over all PELDOR time traces by DeerAnalysis³⁹ for duplex XI (**C**) and duplex XII (**D**).

Conclusions

The new spin label **^{1m}Um**, a derivative of uridine, was prepared for RNA spin-labeling. It was incorporated into different RNA structural contexts by solid-phase oligonucleotide synthesis. The spin-labeled RNAs were analyzed by thermal denaturation experiments, CD- and EPR-spectroscopy. The new label **^{1m}Um** was fairly well tolerated in A-form helices, as judged by thermal denaturation experiments. CW-EPR spectra of **^{1m}Um**-labeled RNA duplexes showed limited mobility, indicating that rotation around the single bond, linking the spin label to the uracil, is restricted. **^{1m}Um** also reported on its local environment by CW-EPR and provided information on the transition from RNA hairpins to duplexes. Distances between pairs of **^{1m}Um** spin labels in RNA duplexes, measured by PELDOR, were in close agreement with distances derived from molecular models. The PELDOR measurements showed a strong orientation-dependence, in particular for RNA **XII**, indicating limited motion of the spin label. Therefore, **^{1m}Um** is a promising RNA spin label for extracting accurate distances and obtaining information about orientations using PELDOR. Such information gives insights into both structure and conformational dynamics of the RNA under investigation.

Experimental section

All commercially available reagents were purchased from Sigma-Aldrich or Acros Organics and used without further purification. 2'-O-methyluridine was purchased from Rasayan Inc. USA. All moisture or air sensitive reactions were performed in flame-dried glasswares under a positive pressure of nitrogen. Solvents were distilled and stored over activated 4 Å molecular sieves under nitrogen. Water was purified on a Milli-Q water purification system. Analytical thin layer chromatography (TLC) was performed on silica gel glass plates (Silicycle, ultra-pure silica gel, 60Å, F₂₅₄), TLC visualisation was performed with UV light. Flash-column chromatography was performed on silica gel (Silicycle, 230-400 mesh, 60Å). ¹H-spectra were recorded using deuterated solvents as internal standards on a Bruker Advance 400 spectrometer and are reported in ppm. Residual proton signals from the deuterated solvents were used as references [D₂O (4.81 ppm), d₆-DMSO (2.50 ppm), CDCl₃ (7.26 ppm), for ¹H spectra. ¹³C NMR chemical shifts are reported in reference to undeuterated residual solvent (CDCl₃ (77.0 ppm), d₆-DMSO (39.43 ppm). ³¹P NMR chemical shifts were reported relative to 85% H₃PO₄ as an external standard. Commercial grade CDCl₃ was passed over basic alumina shortly before use. Mass spectrometric analyses of all organic compounds were performed on an ESI-HRMS (Bruker, microTOF-Q) in positive or negative mode.

Compound 1

To a solution of 2'-O-methyluridine (5.0 g, 0.019 mol) in CH₃CN (18 mL) was added iodine (2.94 g, 0.012 mol) and ammonium cerium(IV) nitrate (5.30 g, 0.0097 mol). The resulting solution was heated at 80 °C for 1 h, followed by cooling to 22 °C. The solid was filtered, washed with H₂O (100 mL) and CH₃CN (50 mL), and dried *in vacuo* to yield compound **1** as a white solid (6.4 g, 86%). ¹H NMR (d₆-DMSO): δ 11.69 (s, 1H), 8.53 (s, 1H), 5.79 (d, J = 3.9 Hz, 1H), 5.30 (s, 1H), 5.12 (d, J = 6.3 Hz, 1H), 4.11 (d, J = 5.5 Hz, 1H), 3.86 (d, J = 5.5 Hz, 1H), 3.79 (d, J = 4.4 Hz, 1H), 3.70 (ddd, J = 12.0, 4.6, 2.8 Hz, 1H), 3.57 (ddd, J = 12.1, 4.3, 2.4 Hz, 1H), 3.38 (s, 3H). ¹³C NMR (d₆-DMSO): δ 160.46, 150.09, 144.82, 86.55, 84.76, 83.02, 69.31, 67.79, 60.25, 59.64, 57.57. HRMS-ESI: m/z calcd. for C₁₀H₁₂IN₂O₆ (M - H)⁻ 382.9746, found 382.9741.

Compound 2

To a solution of 2'-O-methyl-5-iodouridine (6.4 g, 0.017 mol) in DMF (19.2 mL) and pyridine (19.2 mL) was added *tert*-butyldimethylsilyl chloride (7.53 g, 0.050 mol) and imidazole (3.40 g, 0.050 mol). After stirring at 22 °C for 16 h, the solvent was removed under reduced pressure and the residue was dissolved in EtOAc (200 mL) and H₂O (100 mL) was added. The EtOAc layer was separated and washed with H₂O (2x100 mL). The organic layer was dried over Na₂SO₄, filtered and the solvent evaporated *in vacuo*. The crude product was purified by flash column chromatography (silica gel) using a gradient elution (EtOAc:pet. ether; 10:90 to 15:85) to give compound **2** as a white solid (8.9 g, 87% yield). ¹H NMR (CDCl₃): δ 8.64 (s, 1H), 8.06 (s, 1H), 5.99 (d, J = 4.5 Hz, 1H), 4.23 (t, J = 4.8 Hz, 1H), 4.09 – 4.01 (m, 1H), 3.97 (dd, J = 11.7, 1.8 Hz, 1H), 3.76 (dd, J = 11.7, 1.8 Hz, 1H), 3.67 (t, J = 4.7 Hz, 1H), 3.46 (s, 3H), 0.98 (s, 9H), 0.91 (s, 9H), 0.19 (d, J = 1.6 Hz, 6H), 0.10 (d, J = 7.9 Hz, 6H). ¹³C NMR (CDCl₃): δ 159.93, 149.99, 144.40, 87.50, 85.65, 84.15, 69.84, 69.00, 62.26, 58.52, 26.56, 25.92, 18.91, 18.35, -4.38, -4.55, -4.71, -4.81. HRMS-ESI: m/z calcd. for C₂₂H₄₀IN₂O₆Si₂ (M - H)⁻ 611.1475, found 611.1443.

Compound 3

Palladium (II) acetate (74 mg, 0.33 mmol), PPh₃ (154 mg, 0.590 mmol) and anhydrous triethylamine (3.64 mL, 26.11 mmol) were combined in anhydrous DMF (10.8 mL) and stirred at 64 °C until an intense red colour developed. A solution of compound **5** (2 g, 3.26 mmol) and vinylacetate (15.17 g, 176.25 mmol) in anhydrous DMF (16.50 mL) was added and the stirring maintained at 64 °C for 17 h. The resulting precipitate of palladium was removed by filtration, the filtrate evaporated to dryness and H₂O (75 mL) was added to the residue. The aqueous mixture was extracted with CH₂Cl₂ (3x100 mL). The organic layer was dried over Na₂SO₄, filtered, the solvent evaporated *in vacuo* and the crude product was purified by flash column chromatography (silica gel) using a gradient elution (CH₂Cl₂:pet. ether; 5:95 to 10:90) to give compound **3** as a white solid (903 mg, 54% yield). ¹H NMR (CDCl₃): δ 8.64 (s, 1H), 8.06 (s, 1H), 5.99 (d, J = 4.5 Hz, 1H), 4.23 (t, J = 4.8 Hz, 1H), 4.09 – 4.01 (m, 1H), 3.97 (dd, J = 11.7, 1.8 Hz, 1H), 3.76 (dd, J = 11.7, 1.8 Hz, 1H), 3.67 (t, J = 4.7 Hz, 1H), 3.46 (s, 3H), 0.98 (s, 9H), 0.91 (s, 9H), 0.19 (d, J = 1.6 Hz, 6H), 0.10 (d, J = 7.9 Hz, 6H). ¹³C NMR (CDCl₃): δ 161.91, 159.99, 150.03, 149.56, 144.39, 137.03, 128.18, 117.13, 112.96, 87.49, 85.64, 85.22, 84.15, 83.91, 69.80, 69.03, 62.28, 58.52, 58.46, 26.56, 26.30, 25.93, 18.91, 18.82, 18.37, -4.36, -4.57, -4.71, -4.82, -4.98, -5.10. HRMS-ESI: m/z calcd. for C₂₄H₄₃N₂O₆Si₂ (M - H)⁻ 511.2665, found 511.2643.

Compound 4

Compound **3** (3.72 g, 0.00725 mol), *N*-methylmorpholine-N-oxide (2.13 g, 0.0181 mol), and OsO₄ (0.0276 g, 0.000109 mol) were stirred in a solution of acetone-H₂O-tBuOH (4:1:1, 30 mL) at 22 °C for 22 h. The reaction mixture was partitioned between EtOAc (300 mL) and H₂O (150 mL). The aqueous layer was extracted with EtOAc (2x100 mL). The combined organic layers were dried over Na₂SO₄, filtered,

the solvent evaporated *in vacuo* and the crude product was purified by flash column chromatography (silica gel) using a gradient elution (MeOH:CH₂Cl₂; 0:100 to 2:98) to give compound **4A**, the diol intermediate, as a white solid (3.17 g, 80% yield). ¹H NMR (CDCl₃): δ 9.07 (s, 1H), 7.65 (d, *J* = 7.9 Hz, 1H), 6.07 – 5.89 (m, 1H), 4.77 – 4.44 (m, 1H), 4.23 (dd, *J* = 10.0, 5.0 Hz, 1H), 4.07 – 3.97 (m, 1H), 3.91 (ddd, *J* = 11.5, 5.5, 2.8 Hz, 1H), 3.87 – 3.79 (m, 1H), 3.79 – 3.63 (m, 3H), 3.46 (dd, *J* = 14.5, 2.8 Hz, 3H), 1.11 – 0.75 (m, 18H), 0.27 – 0.05 (m, 12H). ¹³C NMR (CDCl₃): δ 163.58, 163.45, 149.92, 149.87, 138.32, 138.19, 113.76, 87.84, 87.71, 85.43, 83.46, 83.37, 70.20, 70.07, 69.98, 69.73, 65.79, 62.70, 62.56, 58.48, 58.45, 26.27, 25.93, 18.77, 18.36, -4.40, -4.43, -4.55, -5.06, -5.10, -5.13. HRMS-ESI: calcd. for C₂₄H₄₆N₂O₈Si₂Na (M + Na)⁺ 569.2685, found 569.2688.

To a solution of **4A** (790.0 mg, 1.444 mmol) in CH₂Cl₂ (50 mL) and H₂O (5 mL) at 22 °C was added NaIO₄ (4.015 g, 18.77 mmol) and the resulting mixture was stirred vigorously for 16 h. The reaction was diluted with H₂O (25 mL) and extracted with CH₂Cl₂ (3x50 mL). The combined organic layers were dried over Na₂SO₄, filtered and the solvent evaporated *in vacuo*. The crude product was purified by flash column chromatography (silica gel) using a gradient elution (CH₂Cl₂:pet.ether; 50:50 to 100:0) to give compound **4** as a white solid (610 mg, 82% yield). ¹H NMR (CDCl₃): δ 10.01 (s, 1H), 8.90 (s, 1H), 8.48 (s, 1H), 6.03 (d, *J* = 4.6 Hz, 1H), 4.25 (t, *J* = 4.7 Hz, 1H), 4.08 (dt, *J* = 4.6, 2.4 Hz, 1H), 3.96 (dd, *J* = 11.7, 2.3 Hz, 1H), 3.86 – 3.69 (m, 2H), 3.46 (s, 3H), 0.92 (t, *J* = 6.9 Hz, 19H), 0.13 (dd, *J* = 23.0, 6.1 Hz, 12H). ¹³C NMR (CDCl₃): δ 185.69, 161.74, 149.40, 145.65, 111.81, 88.08, 86.18, 84.24, 69.91, 62.31, 58.57, 26.34, 25.91, 18.82, 18.33, -4.41, -4.52, -5.21, -5.22. HRMS-ESI: m/z calcd. for C₂₃H₄₂N₂O₇Si₂Na (M + Na)⁺ 537.2423, found 537.2432.

Compound 6

To a solution of compound **4** (876.0 mg, 1.701 mmol) and 1,1,3,3-tetramethylisoindoline-5,6-diamine (**5**) (349.0 mg, 1.701 mmol) in MeOH (9 mL) was added K₃Fe(CN)₆ (672.0 mg, 2.041 mmol) and the reaction stirred for 16 h at 22 °C. The reaction mixture was concentrated *in vacuo* and the crude product was purified by flash column chromatography (silica gel) using a gradient elution (CH₂Cl₂:MeOH; 98:02 to 90:10) to give compound **6** as a yellow solid (590.0 mg, 50% yield). ¹H NMR (d₆-DMSO): δ 12.04 (s, 1H), 8.59 (s, 1H), 7.29 (s, 1H), 7.20 (s, 1H), 5.93 (d, *J* = 4.4 Hz, 1H), 4.28 (t, *J* = 5.0 Hz, 1H), 4.04 – 3.75 (m, 4H), 3.39 (d, *J* = 5.0 Hz, 3H), 1.39 (s, 13H), 0.89 (d, *J* = 4.6 Hz, 19H), 0.13 (dd, *J* = 17.6, 2.4 Hz, 12H). ¹³C NMR (d₆-DMSO): δ 161.83, 149.56, 145.62, 143.70, 143.45, 142.45, 139.88, 134.09, 109.73, 104.78, 104.12, 87.23, 84.69, 82.16, 69.66, 62.25, 61.74, 61.60, 57.69, 45.67, 32.59, 32.56, 30.64, 25.96, 25.58, 18.09, 17.76, 11.49, -4.79, -5.01, -5.37, -5.38. HRMS-ESI: m/z calcd. for C₃₅H₅₈N₅O₆Si₂ (M + H)⁺ 700.3920, found 700.3952.

Compound 7

To a suspension of **6** (270.0 mg, 0.39 mmol) in CH₃CN (18 mL) was added NaN₃ (100.0 mg, 1.54 mmol) and the reaction stirred at 22 °C. After 30 min, *m*CPBA (133.0 mg, 0.77 mmol) was added, the reaction mixture stirred for 3 h and concentrated *in vacuo*. The residue was purified by silica gel column chromatography using a gradient elution (CH₂Cl₂:MeOH; 100:0 to 98:2) to give compound **7** as a yellow solid (162.0 mg, 59% yield). ¹H NMR (CDCl₃): δ 11.45 (br s), 9.90 (br s), 8.92 (br s), 8.08 (br s), 7.98 (br s), 7.26 (br s), 6.13 (br s), 4.37 (br s), 4.11

(br s), 4.00 (br s), 3.97 (br s), 3.86 (br s), 3.46 (br s), 2.18 (br s), 2.13 (br s), 1.04 (br s), 0.93 (br s), 0.89 (br s), 0.21 (br s), 0.19 (br s), 0.14 (br s), 0.13 (br s). ¹³C NMR (CDCl₃): δ 170.34, 162.59, 149.30, 146.90, 141.72, 136.68, 136.01, 133.89, 131.40, 129.73, 129.15, 127.73, 104.30, 88.24, 86.11, 83.15, 77.55, 77.23, 76.91, 73.48, 69.94, 62.49, 58.17, 31.52, 29.54, 26.03, 25.91, 25.74, 25.63, 25.56, 18.35, 17.97, 8.29, -4.79, -4.82, -5.34, -5.45. HRMS-ESI: m/z calcd. for C₃₅H₅₇N₅O₇Si₂ (M + H)⁺ 715.3791, found 715.3776.

^{Im}U_m

To a solution of compound **7** (320 mg, 0.4475 mmol) in THF (32 mL) was added *tert*-butyl ammonium fluoride (1 M in THF, 1.03 mL, 0.985 mmol) and the solution was stirred at 22 °C for 16 h. The solvent was removed under reduced pressure to give a sticky reddish oil. The crude product was purified by flash column chromatography (silica gel) using a gradient elution (CH₂Cl₂:MeOH; 100:0 to 95:5) to give compound ^{Im}U_m as a yellow solid (175 mg, 80% yield). ¹H NMR (d₆-DMSO): δ 12.45 (br s), 12.00 (br s), 8.77 (br s), 7.90 (br s), 7.71 (br s), 7.54 (br s), 6.00 (br s), 5.74 (br s), 5.22 (br s), 4.17 (br s), 3.95 (br s), 3.74 (br s), 3.65 (br s), 3.42 (br s), 3.32 (br s), 3.17 (br s). ¹³C NMR (d₆-DMSO): δ 161.86, 149.30, 132.60, 130.54, 128.65, 127.76, 86.68, 85.14, 82.82, 68.27, 60.53, 57.57, 55.17. HRMS-ESI: m/z calcd. for C₂₃H₂₉N₅O₇ (M + H)⁺ 487.2061, found 487.2068.

Compound 8

^{Im}U_m (150.0 mg, 0.31 mmol), DMTCI (189.0 mg, 0.56 mmol) and DMAP (4.0 mg, 0.032 mmol) were weighed into a round bottom flask and kept *in vacuo* for 12 h. Pyridine (2.0 mL) was added and the solution was stirred at 22 °C for 3 h, after which MeOH (100 μL) was added. The solvent was removed *in vacuo* and the residue was purified by flash column chromatography (silica gel) using a gradient of (CH₂Cl₂:MeOH; 100:0 to 97:2.5 + 0.5% Et₃N); the column was prepared in 0.5% Et₃N in CH₂Cl₂. Compound **8** was obtained as a yellow solid (195.0 mg, 80.0%). ¹H NMR (CDCl₃): δ 11.32 (br s), 8.91 (br s), 8.69 (br s), 7.56 (br s), 7.49 (br s), 6.78 (br s), 6.09 (br s), 5.33 (br s), 4.50 (br s), 4.50 (br s), 4.20 (br s), 4.13 (br s), 3.71 (br s), 3.60 (br s), 2.98 (br s). ¹³C NMR (CDCl₃): δ 161.97, 157.71, 157.66, 149.08, 148.58, 143.83, 141.07, 135.35, 135.15, 129.52, 129.41, 127.59, 127.11, 126.05, 112.41, 88.12, 86.13, 83.36, 82.81, 68.44, 61.75, 58.59, 54.88, 45.07, 8.81. HRMS-ESI: m/z calcd. for C₄₄H₄₉N₅O₇ (M + H)⁺ 789.3368, found 789.3396.

Compound 9

Diisopropyl ammonium tetrazolide (33.0 mg, 0.19 mmol) and compound **8** (100.0 mg, 0.13 mmol) were dissolved in pyridine (2 mL), the solvent evaporated *in vacuo* and residue kept under vacuum for 17 h. CH₂Cl₂ (3.0 mL) and 2-cyanoethyl *N,N,N',N'*-tetraisopropyl phosphoramidite (115.0 mg, 0.38 mmol) were added. The reaction mixture was stirred at 22 °C for 16 h, diluted with CH₂Cl₂ (10 mL) and washed successively with saturated aq. NaHCO₃ (3x10 mL) and saturated aq. NaCl (2x10 mL). The organic layer was dried over anhydrous Na₂SO₄, filtered and concentrated *in vacuo*. The crude solid was purified by precipitation by first dissolving it in CH₂Cl₂ (0.5 mL), followed by addition of pet. ether (50 mL). The liquid was decanted and the operation repeated three times to furnish phosphoramidite **9** as a pale yellow solid (95 mg, 76%). ¹H NMR (CDCl₃): δ 11.29 (br s), 9.02 (br s), 8.95 (br s), 7.61 (br s), 7.53 (br s),

6.82 (br s), 6.19, 6.10 (br s), 4.70 (br s), 4.54 (br s), 4.39 (br s), 4.25 (br s), 3.66 (br s), 3.54 (br s), 2.71 (br s), 2.45 (br s), 1.47 (br s), 1.35 (br s), 1.24 (br s), 1.13 (br s). ^{31}P NMR (CDCl_3): δ 150.73. HRMS-ESI: m/z: calcd. for $\text{C}_{53}\text{H}_{64}\text{N}_7\text{O}_{10}\text{P}$ ($M + \text{H}$)⁺ 989.4446, found 989.4411.

Oligonucleotide synthesis

RNA oligonucleotides were synthesized on an automated ASM800 DNA/RNA synthesizer (Biosset, Novosibirsk, Russia) by using a trityl-off protocol and phosphoramidites with standard protecting groups on a 1.0 mmol scale, using 1000 Å CPG columns. All commercial phosphoramidites, CPG columns, and solutions were purchased from ChemGenes Corporation (Wilmington, MA). $^{\text{Im}}\text{Um}$ was incorporated into RNA oligoribonucleotides by solid phase synthesis using the previously reported protocol,²⁴ with a slight modification. The activator 5-(benzylthio)-1*H*-tetrazole that is normally used for RNA synthesis was not suitable for $^{\text{Im}}\text{Um}$, as we observed a coupling efficiency of less than 5% (as judged by the change of color during trityl deprotection after coupling of $^{\text{Im}}\text{Um}$ phosphoramidite) when using this reagent. Therefore, 5-(ethylthio)-1*H*-tetrazole, the activator generally used in our laboratory for DNA synthesis, was used instead. The spin-labeled phosphoramidite was incorporated manually into the oligonucleotides by pausing the synthesizer program after completion of the prior cycle, removing the column from the synthesizer, and running the standard activator solution (200 μL) and a solution of the spin-labeled phosphoramidite (0.05 M, 200 μL) in 1,2-dichloroethane back and forth through the column for 10–12 min. After manual coupling, the column was remounted on the synthesizer and the synthesis cycle completed. Upon completion of the synthesis, the oligoribonucleotides were cleaved from the solid support and the nucleobases and the phosphodiesters deprotected in a 1:1 mixture of conc. aqueous NH_3 and 8 M MeNH_2 in EtOH (2 mL) at 65 °C for 40 min. The supernatant was collected, the beads washed three times with a mixture of EtOH:H₂O (1:1, 300 μL), and the combined washings were dried. The 2'-*O*-TBDMS groups were removed by treatment with a mixture of $\text{Et}_3\text{N} \cdot 3\text{HF:DMF}$ (3:1,800 μL) at 55 °C for 1.5 h, followed by addition of H₂O (200 μL). This mixture was transferred to a 50 mL Falcon tube and n-butanol (40 mL) was added and stored at -20 °C for 12 h, centrifuged and the solvent decanted from the RNA pellet. The crude RNA was subsequently purified by 20% denaturing polyacrylamide gel electrophoresis. The RNA oligonucleotide bands were visualized under UV light, excised from the gel, crushed, and eluted from the gel with a Tris buffer (2x10 mL; Tris (10 mM, pH 7.5), NaCl (250 mM), Na₂EDTA (1 mM)). The RNA elutions were filtered through a 0.45 mm cellulose acetate membrane (Whatman) and desalted using a Sep-Pak cartridge (Waters Corporation). The dried oligoribonucleotides were dissolved in sterile H₂O (400 μL) and their final concentrations were calculated according to Beer's law based on UV absorbance of oligoribonucleotides at 260 nm. Extinction coefficients were determined by using the UV WinLab oligoribonucleotide calculator (V2.85.04; Perkin Elmer). Molecular weights of oligoribonucleotides were determined by MALDI-TOF analysis (Bruker, Autoflex III) after calibration with an external standard. UV/vis spectra were recorded on a PerkinElmer Lambda 25 UV/vis spectrometer. CD spectra were recorded on a JASCO J-810 spectropolarimeter at 20 °C with path length of 1 mm (Hellma), 10 scans, scanned from 500 to 200 nm with response of 1 s, data pitch of 0.1 nm, and bandwidth of 1.0 nm.

CW-EPR measurements

CW-EPR spectra were recorded on a MiniScope MS200 spectrometer using 100 kHz modulation frequency, 1.0 G modulation amplitude, and 2.0 mW microwave power. Each spectrum was scanned 100–120 times. The temperature was regulated by a Magnetech temperature controller M01 with an error of ± 0.5 °C. The sample was prepared by dissolving spin-labeled, single-stranded RNA (2.0 nmol) and its complementary strand (2.4 nmol) in phosphate buffer (10 mM phosphate, 100 mM NaCl, 0.1 mM Na₂EDTA, pH 7.0; 10 mL, oligonucleotide final conc. 200 mM). The resulting sample was annealed by using the following protocol: 90 °C for 2 min, 60 °C for 5 min, 50 °C for 5 min, 40 °C for 5 min, 22 °C for 15 min. The samples (10 μL) were placed in a quartz capillary (BLAUBRAND intraMARK) prior to EPR measurements.

PELDOR measurements

The RNA samples for PELDOR measurement were prepared by annealing 10 nmol of each strand with 10 nmol of its complementary strand in phosphate buffer (100 μL , 10 mM, pH 7.0), NaCl (100 mM), and EDTA (0.1 mM), followed by evaporation of the water. The annealed and dried samples were dissolved in 20% ethylene glycol/H₂O (100 μL) before the PELDOR measurements. The dead-time free four-pulse PELDOR sequence was used for all experiments⁴⁰ and carried out on a Bruker Elexsys E580 X-band spectrometer equipped with Flexline MS-3 probe in an Oxford CF935 cryostat and a PELDOR frequency unit. Microwave pulses were amplified by a 1 kW TWT amplifier (ASE 117x). Typical pulse lengths were 32 ns ($\pi/2$ and π) for the probe pulses and 12 ns (π) for the pump pulse. The delay between the first and second probe pulses was varied between 132 and 196 ns in 8 ns steps to reduce contributions from proton modulations. The pulse separation between the second and third probe pulses was 3.0 μs . The frequency of the pump pulse was fixed to the central maximum of the nitroxide powder spectrum to obtain maximum pumping efficiency. The probe frequency was chosen 40–85 MHz above this frequency. This range corresponds to the smallest frequency offset that avoids a strong pump/probe frequency overlap, and therefore large proton modulation artifacts. The 85 MHz offset is the frequency offset that excites the edge of the nitroxide spectrum. All PELDOR experiments were carried out at 50 K.

Acknowledgements

S. Th. S. acknowledges financial support from the Icelandic Research Fund (141062-051). T. F. P. acknowledges financial support by the SFB 902 - Molecular Principles of RNA-based Regulation. We thank Dr. S. Jonsdottir for assistance in collecting analytical data for structural characterization of the new compounds and Dr. Subham Saha for preparation of this manuscript.

References

- 1 Eddy, S. R. *Nat. Rev. Genet.* 2001, **2**, 919–929.
- 2 He, L.; Hannon, G. J. *Nat. Rev. Genet.* 2004, **5**, 522–531.
- 3 Rockman, M. V.; Kruglyak, L. *Nat. Rev. Genet.* 2006, **7**, 862–872.
- 4 Schiemann, O.; Prisner, T. F. *Q. Rev. Biophys.* 2007, **40**, 1–53.
- 5 Klare, J. P.; Steinhoff, H.-J. *Photosynth. Res.* 2009, **102**, 377–390.

- 6 Ding, Y.; Nguyen, P.; Tangprasertchai, N. S.; Reyes, C. V.; Zhang, X.; Qin, P. Z. *Electron Paramagn. Reson.* 2014, **24**, 122-147.
- 7 Duss, O.; Yulikov, M.; Allain, F. H.; Jeschke, G. *Methods Enzymol.*; Woodson, S. A., Allain, F. H. T., Eds.; Academic Press: 2015, **558**, 279-331.
- 8 Endeward, B.; Marko, A.; Denysenkov, V. P.; Sigurdsson, S. T.; Prisner, T. F. *Methods Enzymol.*; Qin, P. Z., Warncke, K., Eds.; Academic Press: 2015, **564**, 403-425.
- 9 Prisner, T. F.; Marko, A.; Sigurdsson, S. T. *J. Magn. Reson.* 2015, **252**, 187-198.
- 10 Jeschke, G. *Annu. Rev. Phys. Chem.* 2012, **63**, 419-446.
- 11 Sowa, G. Z.; Qin, P. Z. *Prog. Nucleic Acid Res. Mol. Biol.*, 2008, **82**, 147-197.
- 12 Sigurdsson, S. T. *Pure Appl. Chem.* 2011, **83**, 677-686.
- 13 Shelke, S. A.; Sigurdsson, S. T. *Struct. Bonding*; Timmel C., Harmer J., Eds.; Springer, Berlin: 2011, **152**, 121-162.
- 14 Shelke, S. A.; Sigurdsson, S. T. *Eur. J. Org. Chem.* 2012, 2291-2301.
- 15 Kamble, N. R.; Granz, M.; Prisner, T. F.; Sigurdsson, S. T. *Chem. Commun.* 2016, **52**, 14442-14445.
- 16 Allerson, C. R.; Chen, S. L.; Verdine, G. L. *J. Am. Chem. Soc.* 1997, **119**, 7423-7433.
- 17 Ramos, A.; Varani, G. *J. Am. Chem. Soc.* 1998, **120**, 10992-10993.
- 18 Edwards, T. E.; Okonogi, T. M.; Robinson, B. H.; Sigurdsson, S. T. *J. Am. Chem. Soc.* 2001, **123**, 1527-1528.
- 19 Qin, P. Z.; Butcher, S. E.; Feigon, J.; Hubbell, W. L. *Biochemistry* 2001, **40**, 6929-6936.
- 20 Kim, N. K.; Murali, A.; DeRose, V. J. *Chem. Biol.* 2004, **11**, 939-948.
- 21 Sicoli, G.; Wachowius, F.; Bennati, M.; Hobartner, C. *Angew. Chem. Int. Ed.* 2010, **49**, 6443-6447.
- 22 Kerzhner, M.; Abdullin, D.; Więcek, J.; Matsuoka, H.; Hagelueken, G.; Schiemann, O.; Famulok, M. *Chem. Eur. J.* 2016, **22**, 12113-12121.
- 23 Edwards, T. E.; Sigurdsson, S. T. *Nat. Protocols* 2007, **2**, 1954-1962.
- 24 Hobartner, C.; Sicoli, G.; Wachowius, F.; Gophane, D. B.; Sigurdsson, S. T. *J. Org. Chem.* 2012, **77**, 7749-7754.
- 25 Barhate, N.; Cekan, P.; Massey, A. P.; Sigurdsson, S. T. *Angew. Chem., Int. Ed.* 2007, **46**, 2655-2658.
- 26 Cekan, P.; Smith, A. L.; Barhate, N.; Robinson, B. H.; Sigurdsson, S. T. *Nucleic Acids Res.* 2008, **36**, 5946-5954.
- 27 Schiemann, O.; Cekan, P.; Margraf, D.; Prisner, T. F.; Sigurdsson, S. T. *Angew. Chem. Int. Ed.* 2009, **48**, 3292-3295.
- 28 Marko, A.; Denysenkov, V.; Margraf, D.; Cekan, P.; Schiemann, O.; Sigurdsson, S. T.; Prisner, T. F. *J. Am. Chem. Soc.* 2011, **133**, 13375-13379.
- 29 Tkach, I.; Pornsuwan, S.; Höbartner, C.; Wachowius, F.; Sigurdsson, S. T.; Baranova, T. Y.; Diederichsen, U.; Sicoli, G.; Bennati, M. *Phys. Chem. Chem. Phys.* 2013, **15**, 3433-3437.
- 30 Gophane, D. B.; Sigurdsson, S. T. *Chem. Commun.* 2013, **49**, 999-1001.
- 31 Gophane, D. B.; Endeward, B.; Prisner, T. F.; Sigurdsson, S. T. *Chem. Eur. J.* 2014, **20**, 15913-15919.
- 32 Asakura, J.; Robins, M. J. *J. Org. Chem.* 1990, **55**, 4928-4933.
- 33 Fujimoto, K.; Matsuda, S.; Takahashi, N.; Saito, I. *J. Am. Chem. Soc.* 2000, **122**, 5646-5647.
- 34 Kittaka, A.; Kuze, T.; Amano, M.; Tanaka, H.; Miyasaka, T.; Hirose, K.; Yoshida, T.; Sarai, A.; Yasukawa, T.; Ishii, S. *Nucleosides Nucleotides* 1999, **18**, 2769-2783.
- 35 Topczewski, J. J.; Kodet, J. G.; Wiemer, D. F. *J. Org. Chem.* 2011, **76**, 909-919.
- 36 R. Kumar, L. I. Wiebe, E. E. Knaus, *Can. J. Chem.* 1994, **72**, 2005-2010.
- 37 Holbrook, S. R.; Kim, S.-H. *J. Mol. Biol.* 1984, **173**, 361-388.
- 38 Andreatta, D.; Sen, S.; Pérez Lustres, J. L.; Kovalenko, S. A.; Ernsting, N. P.; Murphy, C. J.; Coleman, R. S.; Berg, M. A. *J. Am. Chem. Soc.* 2006, **128**, 6885-6892.
- 39 Jeschke, G.; Chechik, V.; Ionita, P.; Godt, A.; Zimmermann, H.; Banham, J.; Timmel, C. R.; Hilger, D.; Jung, H. *Appl. Magn. Reson.* 2006, **30**, 473-498.
- 40 Martin, R. E.; Pannier, M.; Diederich, F.; Gramlich, V.; Hubrich, M.; Spiess, H. W. *Angew. Chem. Int. Ed.* 1998, **37**, 2833-2837.